

Multi-Camera LiDAR Inertial Extension to the Newer College Dataset

Lintong Zhang, Marco Camurri, David Wisth and Maurice Fallon

Abstract— We present a multi-camera LiDAR inertial dataset of 4.5 km walking distance as an expansion of the Newer College Dataset. The global shutter multi-camera device is hardware synchronized with both the IMU and LiDAR. This dataset also provides six Degrees of Freedom (DoF) ground truth poses at LiDAR frequency (10 Hz). Three data collections are described and an example use case of multi-camera visual-inertial odometry is demonstrated. This expansion dataset contains small and narrow passages, large scale open spaces, as well as vegetated areas, to test localization and mapping systems. Furthermore, some sequences present challenging situations such as abrupt lighting change, textureless surfaces, and aggressive motion. The dataset is available at: <https://ori-drs.github.io/newer-college-dataset/>

I. INTRODUCTION

There has been rapid progress in the field of robotic autonomous navigation. High-quality public datasets can propel research and development, allowing consistent evaluation across different algorithms. Our recent Newer College Dataset [1] features a stereo-inertial camera and a dense LiDAR setup, and introduced a novel method of generating accurate high-frequency ground truth poses. In line with the development of cutting-edge sensors, we now present a new handheld device incorporating a synchronized multi-camera device for challenging visual scenarios, and a wide field of view 128 channel LiDAR that can provide even denser point clouds per single scan.

There are several monocular and stereo camera datasets for visual odometry and Simultaneous Localization and Mapping (SLAM) purpose. Some of these datasets contain IMU or LiDAR measurements. A notable example is the KITTI dataset [2] that provides LiDAR, IMU, and stereo camera data with GPS/INS ground truth. EuRoC MAV [3] and TUM VI [4] both offer 6 Degree of Freedom (DoF) ground truth poses, with data for IMU and stereo cameras, but not any LiDAR sensors. For a more detailed comparison, we refer the reader to Table I in our original paper [1]. However, there is very few public dataset that offers multi-camera vision for odometry or SLAM related usage.

Within the field of computer vision, there are a number of public datasets involving multiple cameras. EPFL-RLC [5] dataset used three static HD cameras inside a building to track objects such as pedestrians. WoodScape [6] was the first fisheye autonomous driving dataset with 4 large Fields of View (FoV) cameras. It provided several categories of information including segmentation, depth estimation, and bounding box. These datasets can be used for a variety of

The authors are with the Oxford Robotics Institute, University of Oxford, UK. {lintong, mcamurri, davidw, mfallon}@robots.ox.ac.uk

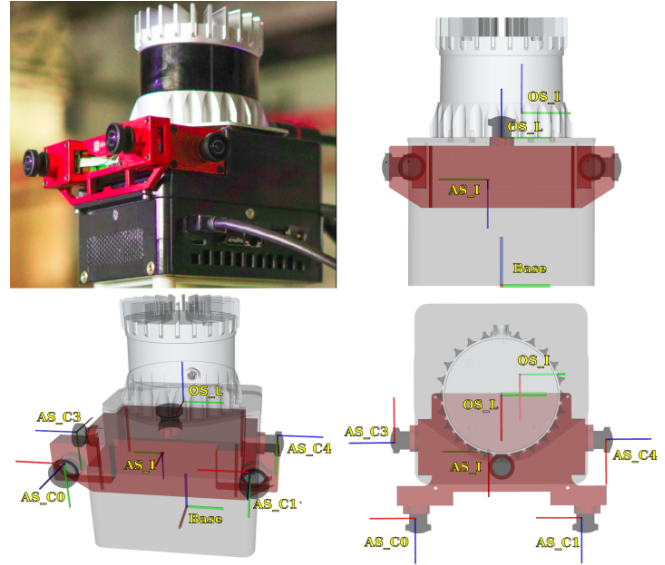


Fig. 1: Our custom built handheld device is on the top left. The other three images are the URDF model with reference frames shown in front, isometric, and top-down views.

computer vision-related research such as object tracking, prediction, and classification, but not for autonomous navigation tasks such as localisation and mapping.

To the best of our knowledge, the only dataset with similar sensors to ours is the Hilti SLAM Challenge dataset [7]. This dataset focused on the construction site environment, providing sparse ground truth poses, with just a few ground truth measurements per sequence. Most sequences are collected in a “stop and go” fashion, where the total station produces a measurement using a reflecting prism during the “stop” periods.

We would like to provide the research community with a comprehensive multi-camera dataset that encompasses vision, LiDAR, inertial measurements, along with high-frequency ground truth poses and accurate prior maps.

II. THE HANDHELD DEVICE

The handheld multi-camera LiDAR inertial device is shown in Fig. 1. The sensors are rigidly attached to a precisely 3D-printed base. A complete URDF model of the device is available as an open source ROS package¹ (see Fig. 1). The Ouster LiDAR is directly mounted above the cameras for a balanced and compact design, so the top facing

¹https://github.com/ori-drs/halo_description

Sensor	Type	Rate	Characteristics
LiDAR	Ouster, OS0-128	10 Hz	128 Channels, 50 m Range 90° Vertical FoV 1024 Horizontal Resolution
Cameras	Alphasense	30 Hz	Global shutter (Infrared) 720×540
LiDAR IMU	ICM-20948	100 Hz	3-axis Gyroscope 3-axis Accelerometer
Camera IMU	Bosch BMI085	200 Hz	Synchronized with cameras

TABLE I: Overview of the sensors in our handheld device.

camera was removed. Tab. I provides an overview of the various sensors.

The multi-camera sensor in our device is the Alphasense Core Development Kit from Sevensense Robotics AG. An FPGA within the Alphasense synchronizes the IMU and four grayscale fisheye cameras – a frontal stereo pair with an 11 cm baseline and two lateral cameras. Each camera has a FoV of $126^\circ \times 92.4^\circ$ and a resolution of 720×540 px. This configuration also produces an overlapping FoV between the front and side cameras of about 36° . The cameras and the embedded cellphone-grade IMU operates at 30 Hz and 200 Hz, respectively. The Ouster OS-0 LiDAR has 128 beams and a 90 degree elevation FoV, which provides a much denser point cloud than the OS1-64 used in the original dataset. Both sensors are cutting-edge devices in mobile robotics research and have recently been used in the DARPA Subterranean Challenge.

Fig. 1 shows the various sensor frames with the following abbreviations:

- Base: The bottom centre of the printed computer case.
- OS_I: The IMU coordinate system in the LiDAR.
- OS_L: The LiDAR coordinate system where the point clouds are read.
- AS_C0, 1, 3, 4: Camera optical frames.
- AS_I: The IMU coordinate system in the Alphasense.

III. DATA COLLECTION

We have collected a variety of datasets at different speeds of walking and turning. The three collections of datasets were gathered at different times of the year and they contain some challenging aspects such as fast motions, aggressive shaking, rapid lighting change, and textureless surfaces. The high frequency ground truth trajectories are also provided using the same method in the original paper, summarized in Sec. IV.

The datasets contain different levels of difficulty and are organized according to the aggressiveness of the motion and the type of scenes observed by the cameras.

Collection 1 - New College:

- *Quad-Easy* (198 s): Two loops in the quad area with a typical walking speed (247 m).
- *Quad-Medium* (190 s): Two loops of brisk walking with cameras pointing in different directions on different occasions (260 m).
- *Quad-Hard* (187 s): Fast walking with aggressive motion, approaches to the walls, and lighting changes (234 m).



Fig. 2: Trajectories for all collections. **Top:** Maths-Easy (green), Maths-Medium (orange), Maths-Hard (purple); **Mid left:** Quad-Easy (green), Quad-Medium (orange), Quad-Hard (purple); **Mid right:** Stairs; **Bot:** Cloister-Easy (green), Park (orange).

- *Stairs* (118 s): Climbing up and down in a narrow stairway with the cameras subject to doors opening and textureless corridor walls (57 m).

Collection 2 - New College:

- *Cloister* (278 s): Two loops of the cloister corridor and the cloister centre quad (429 m).
- *Park* (1567 s): Long experiment of the entire park and two quads with multiple loops. Route corresponds to the original dataset (2396 m).

Collection 3 - Maths Institute:

- *Maths-Easy* (216 s): Outdoor large scale environment with typical walking speed (264 m).
- *Maths-Medium* (176 s): Brisk walking with cameras occasionally turned to face different directions (304 m).

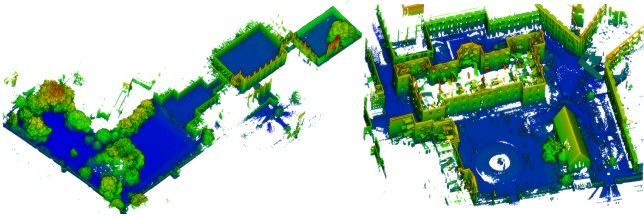


Fig. 3: Ground truth and prior maps. **Left:** New College, Oxford (extended from the original Newer College dataset map); **Right:** Maths Institute, University of Oxford.

- *Maths-Hard* (243 s): Fast walking with aggressive motions, textureless surfaces, rapid rotations and shaking of the device up to 5.5 rad/s (321 m).

In Fig. 2, trajectories for each collection are overlaid on the ground truth map using the method explained in the next section. A video example displaying four camera streams and the point cloud of the cloister sequence can be viewed at <https://youtu.be/tGXNSImQOb0>.

IV. GROUND TRUTH

The prior map and ground truth pose generation process use the same method described in [1]. We use a survey-grade 3D imaging laser scanner, Leica BLK360, to scan the entire environment. As shown in Fig. 3, we further extend the prior map of New College and provide an additional map for the Maths Institute. Group truth poses are determined by registering each LiDAR scan to the prior map using an approach based on the Iterative Closest Point method. The poses are expressed in the “Base” frame shown in Sec. II.

V. CALIBRATION

Similarly to the original stereo camera LiDAR dataset, we use the open source camera and IMU calibration toolbox Kalibr [8] to compute the intrinsic calibration of the Alphasense cameras as well as their extrinsics. We perform spatio-temporal calibration between the cameras and the two IMUs embedded in the Alphasense and the Ouster sensor. The calibration target is 6×6 April grids and each tag size is 8.8 cm. The calibration settings use the pinhole projection model with equidistant distortion. All cameras are calibrated with the IMU, starting with the frontal stereo cameras, then the individual lateral cameras. Since the collections were carried out at different times of the year, we provide a set of calibration files corresponding to each dataset collection.

A. Synchronization

The recording computer, Intel NUC, is modified to support dual Ethernet ports with hardware timestamp capability. The Ouster LiDAR and Alphasense are synchronized with the NUC using the Precision Time Protocol (PTP), which achieves sub-microsecond accuracy.

Further details about the Alphasense synchronization can be found at its Github page². The detailed synchronization

²https://github.com/sevensense-robotics/alphasense_core_manual

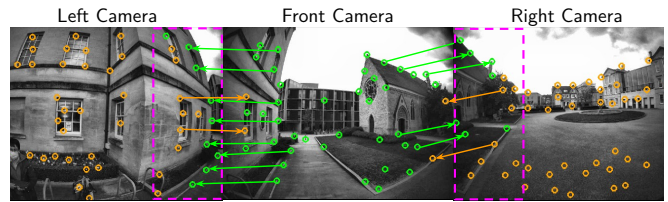


Fig. 4: VILENS-MC takes advantage of any overlapping image regions (purple rectangles) in a multi-camera setup to track features across cameras. This increases feature track length and avoids tracking the same feature independently in different cameras. The arrows indicate features being tracked from one image to another.

procedure for Ouster LiDAR can be found in the software manual³ (Section 16 “PTP Quickstart Guide”).

VI. EXAMPLE USAGE

To demonstrate one usage of the dataset and the advantage of multi-sensor synchronization, we compared three visual-inertial odometry methods, with reference to LiDAR-generated ground truth.

The first is a multi-camera visual-inertial odometry system (VILENS-MC) [9], developed by the authors. VILENS-MC is based on factor graph optimization which estimates motion by using all cameras simultaneously while retaining a fixed overall feature budget. VILENS-MC introduced cross camera feature tracking as shown in Fig. 4, and focuses on motion tracking in challenging environments by leveraging this multi-camera dataset. Many sequences in this dataset, such as Maths-Hard, Quad-Hard or Stairs, would cause classic stereo inertial odometry approaches to fail. As an example, Fig. 5 shows the trajectories estimated by OpenVINS [10], ORBSLAM-3 [11] and VILENS-MC for the Maths-Hard dataset.

VII. CONCLUSION

In this paper, we presented an extension of Newer College Vision and LiDAR dataset. By leveraging a highly accurate and detailed prior map, we provided accurate high-frequency 6 DoF ground truth poses, which distinguishes our dataset from existing ones. We combined a cutting edge multi-camera device and a dense 3D LiDAR sensor to provide challenging scenarios, which are considered difficult for current robotic navigation systems. The paper also illustrated an example use case of multi-camera visual inertial odometry. We hope this dataset can propel researchers to further push the boundaries of autonomous navigation by demonstrating how algorithms can become more robust when taking into account challenging scenarios.

ACKNOWLEDGMENT

The authors would like to thank the members of the Oxford Robotics Institute (ORI) who helped with the creation of this dataset release, especially Wayne Tubby. We also

³<https://data.ouster.io/downloads/software-user-manual/software-user-manual-v2p0.pdf>

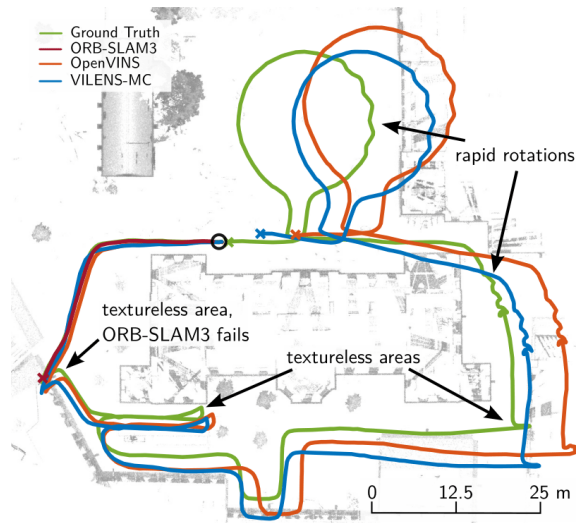


Fig. 5: Top-down view of Maths-Hard dataset comparing the estimated trajectory of ORB-SLAM3, OpenVINS, and VILENS-MC against the ground truth. A black circle marks the start of the trajectory, while colored crosses indicate the last pose of each trajectory. A textureless area, where multiple cameras were facing towards walls was a cause of failure for the stereo odometry methods.

thank the personnel of New College for facilitating our data collection.

This research was supported by the Innovate UK-funded ORCA Robotics Hub (EP/R026173/1) and the EU H2020 Project THING. Maurice Fallon is supported by a Royal Society University Research Fellowship.

REFERENCES

- [1] M. Ramezani, Y. Wang, M. Camurri, D. Wisth, M. Mattamala, and M. Fallon, "The Newer College Dataset: Handheld LiDAR, Inertial and Vision with Ground Truth," in *2020 IEEE/RSJ International Conference on Intelligent Robots and Systems (IROS)*, 2020, pp. 4353–4360.
- [2] A. Geiger, P. Lenz, C. Stiller, and R. Urtasun, "Vision meets robotics: The kitti dataset," *The International Journal of Robotics Research*, vol. 32, no. 11, pp. 1231–1237, 2013.
- [3] M. Burri, J. Nikolic, P. Gohl, T. Schneider, J. Rehder, S. Omari, M. W. Achtelik, and R. Siegwart, "The EuRoC micro aerial vehicle datasets," *International Journal of Robotics Research (IJRR)*, 2016.
- [4] D. Schubert, T. Goll, N. Demmel, V. Usenko, J. Stückler, and D. Cremers, "The TUM VI Benchmark for Evaluating Visual-Inertial Odometry," in *IEEE/RSJ International Conference on Intelligent Robots and Systems (IROS)*, 2018, pp. 1680–1687.
- [5] T. Chavdarova and F. Fleuret, "Deep Multi-camera People Detection," in *IEEE International Conference on Machine Learning and Applications (ICMLA)*, 2017, pp. 848–853.
- [6] S. Yogamani, C. Hughes, J. Horgan, G. Sistu, S. Chennupati, M. Uricar, S. Milz, M. Simon, K. Amende, C. Witt, H. Rashed, S. Nayak, S. Mansoor, P. Varley, X. Perrotton, D. Odea, and P. Pérez, "WoodScape: A Multi-Task, Multi-Camera Fisheye Dataset for Autonomous Driving," in *2019 IEEE/CVF International Conference on Computer Vision (ICCV)*, 2019, pp. 9307–9317.
- [7] M. Helmberger, K. Morin, N. Kumar, D. Wang, Y. Yue, G. Cioffi, and D. Scaramuzza, "The Hilti SLAM Challenge Dataset," *arXiv preprint arXiv:2109.11316*, 2021.
- [8] J. Rehder, J. Nikolic, T. Schneider, T. Hinzmann, and R. Siegwart, "Extending Kalibr: Calibrating the extrinsics of multiple IMUs and of individual axes," in *IEEE International Conference on Robotics and Automation (ICRA)*, 2016, pp. 4304–4311.
- [9] L. Zhang, D. Wisth, M. Camurri, and M. Fallon, "Balancing the budget: Feature selection and tracking for multi-camera visual-inertial odometry," *IEEE Robotics and Automation Letters*, vol. 7, no. 2, pp. 1182–1189, 2022.
- [10] P. Geneva, K. Eickenhoff, W. Lee, Y. Yang, and G. Huang, "OpenVINS: A Research Platform for Visual-Inertial Estimation," in *IEEE/RSJ International Conference on Intelligent Robots and Systems (IROS)*, 2020, pp. 4666–4672.
- [11] C. Campos, R. Elvira, J. J. G. Rodríguez, J. M. M. Montiel, and J. D. Tardós, "ORB-SLAM3: An accurate open-source library for visual, visual-inertial, and multimap SLAM," *IEEE Transactions on Robotics (TRO)*, pp. 1–17, 2021.